Fire Safety Journal 140 (2023) 103858

Contents lists available at ScienceDirect

Fire Safety Journal

journal homepage: www.elsevier.com/locate/firesaf

Convective heat transfer correlation for a single surrogate firebrand and a simplified firebrand pile on a flat plate using naphthalene sublimation in heated air flow

Savannah S. Wessies *, Jiann C. Yang

National Institute of Standards and Technology, 100 Bureau Dr., Gaithersburg, 20899, MD, USA

ARTICLE INFO

Keywords:
Wildfires
Heat transfer
Firebrands
Convection

ABSTRACT

Previous studies have shown that most structure ignitions in wildland urban-interface fires are due to firebrand deposition and ignition. The heat transfer mechanisms involved in firebrand deposition need further study and characterization for better understanding of the firebrand ignition process. In particular, convective heat transfer correlations over a single firebrand and a pile of firebrands are lacking. Using the heat-mass transfer analogy, naphthalene sublimation experiments were conducted to determine convective heat transfer correlations for a single naphthalene cylinder (a surrogate firebrand) and an idealized three-firebrand pile resting on flat plates from mass loss measurements. These experiments were conducted in a wind tunnel using a heated (50 °C) or room temperature air flow (0.5 m/s to 2.1 m/s). There was good agreement between the Nusselt number correlation obtained using heated air and results with unheated airflows. Experiments using heated airflow reduced the experimental run times and uncertainty in mass loss measurements significantly. In general, the single firebrand had higher Nusselt numbers than the individual firebrands in the pile. In the three-firebrand pile, the firebrand at the top of the pile exhibited the highest heat transfer. The naphthalene sublimation technique can be easily extended to obtain convective heat transfer correlations for various firebrand geometries and configurations.

1. Introduction

In wildland-urban interface fires, recent post-fire investigations have shown that the majority of home ignitions are caused by firebrands [1–3]. These structure ignitions occur in a three step process: firebrand generation, transport, and deposition/ignition. The firebrands can take many forms depending on the source material where they were generated. Often small pieces of branches or twigs break off of a larger plant to form firebrands that are nearly cylindrical in shape [4,5]. After traveling away from the generation point, the firebrands can then land on various substrates and possibly initiate an ignition event. This ignition process due to firebrand deposition is being studied and modeled by a variety of researchers [5–10]; however, there are some gaps when it comes to modeling the heat transfer. Firebrands experience conductive, radiative, and convective losses when they are deposited on a substrate. With regards to the convective heat transfer, we might assume that the cylindrical firebrands are resting on a substrate. In more traditional terms, we might say a cylinder resting on a flat plate. However, to the authors' knowledge, there are no correlations for the convective heat transfer from a hot cylinder resting on unheated flat plate in the literature. This scenario would represent a single firebrand landing on a substrate; however, there are often multiple firebrands that collect on a surface forming piles [11,12]. Accounting the heat transfer from a firebrand pile would involve quantifying the amount of heat transfer from the pile to the environment/substrate and the heat transfer from individual firebrands to other firebrands within the pile. Specifically with regards to convective heat transfer, the location of the firebrand within the pile and with respect to the wind direction could greatly change the amount of convective heat transfer a given firebrand experiences. By studying the convective heat transfer of a single firebrand on a surface and of a pile of firebrands, we can improve our understanding and modeling of the heat transfer occurring in firebrand deposition scenarios.

Isolating the convective portion of the heat transfer in a reacting system is non-trivial. For more than seventy years, naphthalene sublimation has been used to characterize convective heat and mass transfer in various geometries. With this technique, the surface or part of it is coated with or formed from naphthalene which sublimes at room temperature. As air flows over the naphthalene surface, mass

* Corresponding author.
E-mail addresses: savannah.wessies@nist.gov (S.S. Wessies), jiann.yang@nist.gov (J.C. Yang).

https://doi.org/10.1016/j.firesaf.2023.103858
Received 5 June 2023; Accepted 4 July 2023
Available online 7 July 2023
0379-7112/Published by Elsevier Ltd.

is transferred away from the surface as the naphthalene sublimes. This is similar to how heat would transfer from a surface to the air flowing past it in a heat transfer scenario [13]. Using the heat/mass transfer analogy, the mass transfer can be related to the convective heat transfer. This mass-heat analogy allows for purely convective heat transfer to be quantified for complex geometries and boundary conditions. The general procedure for naphthalene experiments is described below [14]:

1. Fabricate the naphthalene test specimen.
2. Measure and record either the initial mass or surface profile of the naphthalene specimen
3. Place the naphthalene specimen in the test apparatus. Conduct the test with the naphthalene test specimen in place and exposed to the test conditions (e.g., air flow).
4. Remove the naphthalene test specimen from the test apparatus. Measure and record the final mass or surface profile of the naphthalene specimen.
5. Using the recorded pre- and post-test measurements of the naphthalene specimens, calculate the mass transfer coefficient or other desired quantities (Sherwood number, heat transfer coefficient, Nusselt number).

There are many different methods to reduce the mass and surface profile data to obtain the transfer coefficients. A procedure for determining the average heat transfer coefficients and Nusselt numbers from mass measurements is detailed below. Eq. (1) describes how the mass transfer of naphthalene relates to the mass transfer coefficient and the mass fraction of naphthalene, where $\dot{m}''$ is the mass flux at the surface, h_m is the mass transfer coefficient, Y_s is the mass fraction of naphthalene vapor at the surface, and Y_∞ is the mass fraction of naphthalene vapor in the far field. Generally, the mass fraction of naphthalene in the far field is assumed to be negligible.

$$\dot{m}'' = h_m(Y_s - Y_\infty) \approx h_m Y_s \tag{1}$$

Using the experimentally determined pre- and post-test mass data, the average mass flux from the surface of the naphthalene over the course of the test can be found using Eq. (2), where Δm is the change in mass over the testing period, A is the surface area, and t is the test time.

$$\dot{m}'' = \frac{\Delta m}{A \Delta t} \tag{2}$$

It is implicitly assumed in Eq. (2) that A is constant and does not change significantly over the course of the test duration. The mass fraction of naphthalene at the surface is proportional the density fraction of naphthalene at the surface, $Y_s \approx \frac{\rho_s}{\rho_{total}}$, where ρ_s is the density of naphthalene vapor at the surface and ρ_{total} is the total density of the gas the naphthalene is subliming into. The partial pressure of naphthalene at the surface is taken to be the equilibrium vapor pressure of naphthalene. Using the ideal gas law (P = ρRT), we can relate the partial pressure of naphthalene at the surface to the density of naphthalene at the surface. The vapor pressure of naphthalene has a strong dependence on temperature, and there are correlations in the literature relating the variation of vapor pressure of naphthalene with temperature. One of the more widely used correlations was developed in 1975 by Ambrose et al. [15]. The correlation, which is valid between 263 K and 343 K, is presented in Eq. (3). Temperature, T, and pressure, P, are in K and Pa, respectively. $E_s(x)$ is a Chebyshev polynomial in x of degree s, where $x = [2T - (T_{max} + T_{min})]/(T_{max} - T_{min})$. In these equations, $a_0 = 301.6247$, $a_1 = 791.4937$, $a_2 = -8.2536$, $a_3 = 0.4043$, $T_{max} = 344$ K, and $T_{min} = 230$ K. An expanded form of Eq. (3) is shown in Eq. (4) in terms of x.

$$T\ log_{10}(P) = \frac{1}{2}a_0 + \sum_{s=1}^{3} a_s E_s(x) \tag{3}$$

$$T\ log_{10}(P) = \frac{1}{2}a_0 + a_1 x + a_2(2x^2 - 1) + a_3(4x^3 - 3x) \tag{4}$$

Once the mass fraction of naphthalene vapor at the surface is known and the naphthalene mass flux is experimentally measured, Eq. (1) can be used to determine the mass transfer coefficient for the given experimental configuration and conditions. With the known mass transfer coefficient, h_m, the heat transfer coefficient, h, can be calculated using the heat and mass transfer analogy, $h = h_m c_p$, where c_p is the specific heat capacity of the convecting gas. The Nusselt number (Nu = hD/k) can then be determined, where D is the diameter of the cylinder and k is the thermal conductivity of the convecting gas.

In this paper, we will describe the experimental procedure and data reduction using the mass loss measurement approach to determine the heat transfer coefficients of a surrogate deposited firebrand (cylinder resting on a flat plate) and the most basic pile configuration of three surrogate firebrands deposited on a surface. The majority of naphthalene sublimation experiments in the literature are conducted at room temperature (approximately 20 °C to 25 °C). However, at room temperature, the experiments must be conducted for longer periods of time to ensure sufficient mass loss. By increasing the temperature of the freestream air, the same amount of mass loss would occur over a shorter period of time. This paper explores the effects of increasing the temperature of the air flowing for characterizing the convective heat transfer. Nusselt number correlations for the surrogate firebrand (cylinder resting on a flat plate) and a pile of three surrogate firebrands resting on a flat plate in cross flow will be presented.

2. Experimental setup and methodology

The experimental setup consists of a wind tunnel equipped with a blower, a heating section, a scale with a 0.001 g resolution, and a data acquisition system. The experimental system is depicted in Fig. 1. The blower was connected to a variac to control the flow speed. Freestream velocities ranged between approximately 0.5 m/s and 2.0 m/s. Immediately after the blower, the wind tunnel converged into a 100 mm × 100 mm square cross-section and the heating section, which was equipped with a temperature controller to regulate the air flow temperature in the wind tunnel. Following the heating section (length 50 cm), the flowing air passed through a series of horse hair filters and fine mesh screens to flatten the flow profile. At the start of the test section, there was approximately 2% variation in the flow velocity within 25 mm on either side of the center line. A k-type thermocouple was installed in the wind tunnel at the inlet of the test section to ensure that the air in the test section was at the desired temperature.

In the test section, two small holes were drilled in the bottom of the wind tunnel wall to allow for mass measurement during testing. The scale was raised to rest below the bottom surface of the wind tunnel test section, and two aluminum supports (117 mm length) resting on the scale reached into the wind tunnel through the drilled holes. The aluminum supports are pictured resting on the scale in Fig. 1. These supports and a 90.2 mm × 152.4 mm piece of 3 mm thick polycarbonate formed a platform that rested 50.8 mm below the top surface of the test section in the center of the tunnel (see Fig. 2). The short side of the platform (90.2 mm) was perpendicular to the flow and centered across the width of the test section. There was a small gap between the platform edge and the sides of the wind tunnel. There were three 0.127 mm diameter, k-type thermocouples located near the platform (approximately 3 mm above the platform and 50 mm apart). During the heated tests, the variation between the thermocouples was about 1 °C to 2 °C. When room temperature air was used, the temperature variation across the platform was between 0.2 °C to 0.5 °C. Additionally, a pitot tube was situated 25.4 mm from the top of the wind tunnel downstream of the platform. The scale in these experiments had a RS232 connection for continuous mass measurements throughout the experiments. During the experiment, the surrogate naphthalene firebrands were weighed at various time intervals. After the mass measurements were recorded, the

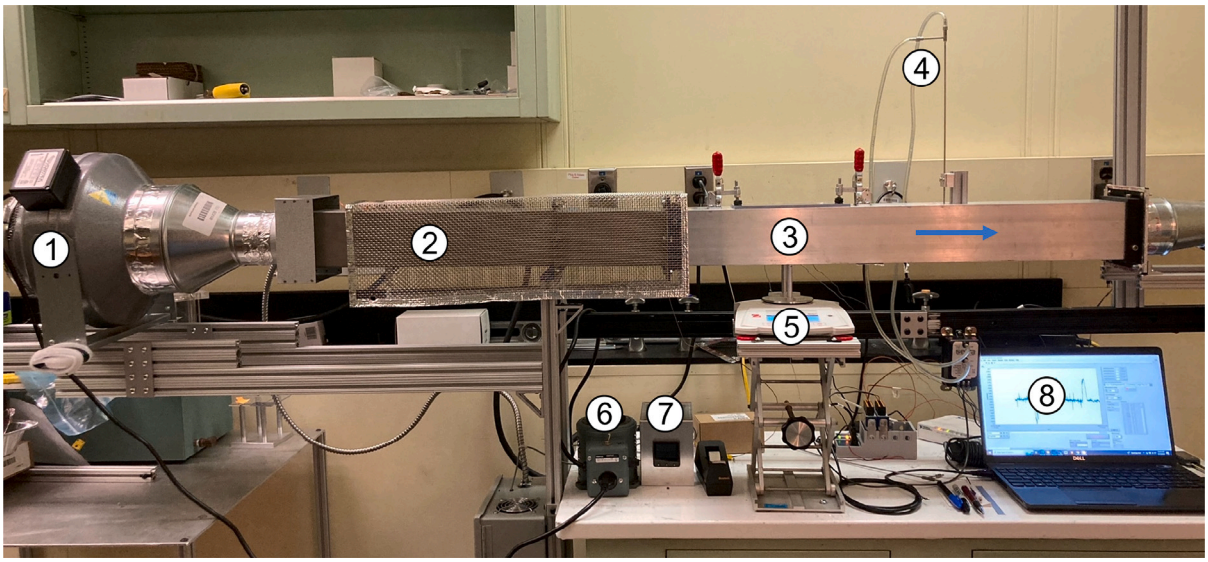

Fig. 1. Schematic of the experimental system. A wind tunnel with a blower (1) connected to the inlet. The air is pushed through the heating section (2) before entering the test section (3). A blue arrow is used to indicate the air flow direction. A pitot tube (4) monitors the flow speed. A scale (5) is located underneath the test section. A variac (6) and a temperature controller (7) are used to control the flow speed and temperature, respectively. The data acquisition system is located at (8). (For interpretation of the references to color in this figure legend, the reader is referred to the web version of this article.)

data collection was terminated. Velocity, temperature, and mass data were collected in each experiment via a data acquisition system.

The surrogate firebrands (naphthalene specimens) in these sublimation experiments took the form of a cylinder with a diameter of 6.35 mm and 50.8 mm long. These dimensions are within the range of firebrands produced in wildland fires. Silicone molds were formed and used to fabricate the naphthalene cylinders. The inside surface of the silicone molds is smooth and shiny, and this finish transfers to the molded naphthalene. According to the literature, a "glasslike smoothness" is desired for the naphthalene specimen's surface [13]. To generate the naphthalene specimens, solid naphthalene is melted and poured into the silicone molds. After the naphthalene cools and solidifies, the naphthalene cylinder is removed from the mold. The cylinder was placed on its rounded side in contact with the platform during an experiment (refer to Fig. 2). Small grooves along the length of the platform allowed for repeatable placement of the surrogate firebrands across replicate tests. For the individual firebrand experiments, a single naphthalene cylinder was placed on the platform in the first groove (25 mm from the leading edge). The cylinder was positioned with its length parallel to the short side of the platform. Similarly for the pile tests, one cylinder was placed in each of the first two grooves, and a third rested on top of the other two surrogate firebrands.

To perform an experiment, the wind tunnel and heating section were first turned on at least thirty minutes prior to testing. This warm up time allowed the air flow to reach a uniform temperature within the test section. During this time, the naphthalene cylinders were fabricated using the silicone molds. Before placing the naphthalene cylinder(s) in the test section, each naphthalene piece was weighed on a scale with a resolution of 0.001 g, and the initial mass was recorded. Immediately following, data collection in the wind tunnel was initiated, and the cylinders were placed in the wind tunnel. The experiment was then allowed to run for a prescribed amount of time. To get the mass loss of the individual members within the pile, an external scale (0.001 g resolution) was used to measure each surrogate firebrand pre- and post-test. This allowed for the calculation of Nusselt numbers for the different positions in the pile. These external mass measurements were also taken for the single tests.

To explore the effect of the air temperature on naphthalene sublimation, the wind speed and air temperature were varied in the single firebrand configuration. Nominally three air flow conditions were tested when the air temperature was held at 50 °C and at room temperature (23 °C). The freestream velocities, U, were approximately 0.6 m/s, 1 m/s, and 2 m/s with some variation among tests. For the heated flow, these velocities correspond to Reynolds numbers ($Re = UD/\nu$) of approximately 196, 391, and 725 when using the diameter of the cylinder, D, as the characteristic length and ν is the kinematic viscosity. With room temperature air at nominally the same freestream velocities, the resulting Reynolds numbers based on the naphthalene cylinder's diameter were 250, 436, and 841. For the heated flow experiments, room temperature naphthalene cylinders were placed in the wind tunnel under a 50 °C air flow. With a room temperature cylinder placed in the heated air flow, there is a delay before the cylinder reaches the temperature of the flow. During this preheating time, the naphthalene does not sublimate at the same rate as later in the test once it has reached the desired temperature. Experiments with a thermocouple embedded in the center of the naphthalene cylinder showed the cylinders took just under ten minutes for the internal temperature of the cylinder to equilibrate with the flow temperature. With this in mind, Nusselt numbers were calculated for the first ten minutes of testing and then for the remaining time period to investigate how the preheating period affects the transfer coefficients. This preheating time was not necessary for the room temperature tests as the naphthalene cylinders and the air flow were at the same temperature. The room temperature tests were collected at much longer time scales (hours rather than minutes) to produce sufficient mass loss. At least six experiments were conducted for each of the heat flow conditions, and triplicates were conducted for each flow condition with the room temperature air flow.

In addition to the singular firebrand configuration, experiments were conducted with three surrogate firebrands in a pile. These experiments were only conducted with the heated (50 °C) airflow. Four different freestream velocities were used for the pile configuration: 0.5 m/s, 1.1 m/s, 1.9 m/s, and 2.1 m/s. These corresponded to Reynolds numbers of 182, 404, 696, 767 based on the diameter of the surrogate firebrand. Measurements were taken for each naphthalene cylinder allowing for heat transfer characterization of the individual firebrands and of the global pile. Data for the heat transfer coefficient was collected for at least ten minutes after the initial preheating period. For the lower flow tests ($Re \approx 182$), an additional ten minutes of data was collected to minimize the errors associated with lower mass loss per

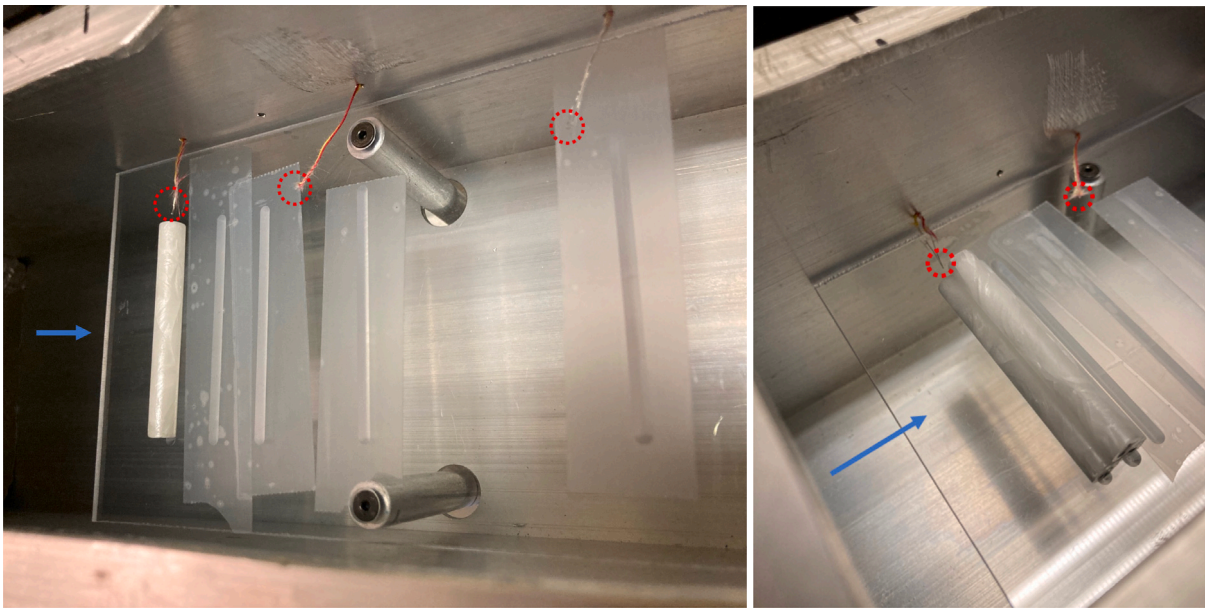

(a) (b)

Fig. 2. Surrogate naphthalene firebrands placed on the platform in the test section in two configurations: (a) single and (b) pile of three. This is a top down view. The blue arrow indicates the direction of the flow. The red dashed circles mark the locations of the thermocouples during testing. (For interpretation of the references to color in this figure legend, the reader is referred to the web version of this article.)

test. Four experiments were conducted for each flow condition in the pile configuration. In the pile tests, after the initial preheating time of ten minutes, the experiments were conducted for ten minutes.

3. Results and discussion

In these experiments, we are interested in the convective heat transfer characterization, so the results will be presented in dimensionless form using the Nusselt number (hD/k), where D is the diameter of the naphthalene cylinder and k is the thermal conductivity of the air.

3.1. Single surrogate firebrand

The single surrogate firebrand experiments were designed to characterize the convective heat transfer from a single firebrand resting on a surface and also explore the effects of using a heated airflow in naphthalene sublimation. First we considered the preheating time due to placing a room temperature object into a heated air flow. The results can be divided into two sections: preheating and data collection. The Nusselt numbers were calculated for both the preheating and actual data collection periods. The values are plotted against the Reynolds number in Fig. 3. At lower velocities, there tended to be less of a difference between the preheat and data collection Nusselt numbers. However there was higher variability between the values for the preheat portion of the experiments compared to the actual data collection portion at the lower velocities. This is particularly evident at Re ≈ 196, where the uncertainty of the mean Nusselt number for the preheating was almost double the uncertainty of the mean Nusselt number for the actual data collection. The uncertainty of the mean was calculated using a 95% confidence interval based on the student's t-distribution. At the highest velocity, there was a distinct difference between the preheat and data collection heat transfer. For Re ≈ 725, the average Nusselt number during preheat was 3.74 ± 0.31 compared to 4.15 ± 0.25 during the data collection period.

In addition to looking at the average Nu and variability, we can compare the correlations between the data. The line of best fit for the data was assumed to have the following form, $Nu = aRe^b$, where a and b are constants. The constants, a and b, were optimized for using scipy.optimize.curve fit with a Levenberg–Marquardt algorithm for the least-squares regression [16]. The correlation for Nusselt number based on Reynolds number was determined for each period (preheating and data collection). The best fit equations are displayed in Fig. 3. At lower Reynolds numbers, the two curve fits are almost the same. However, as higher Reynolds numbers are approached, the preheat correlation predicts lower Nusselt numbers than the data collection correlation. There is a clear difference between the values collected during the initial heating period of the naphthalene cylinders in the heated air flow. For this naphthalene form factor and heated air flow, ten minutes provides sufficient time for the naphthalene to equilibrate to the flow temperature. For other experimental configurations, the preheat time would need to be re-evaluated.

For the single surrogate firebrand configuration, experiments were also conducted at room temperature for similar flow conditions to ensure the validity of the Nusselt number correlation determined in the heated flow tests. Moving forward, only the values for the Nusselt number from the data collection period will be discussed. The Nusselt number results of the individual tests are plotted in Fig. 4. The values from the heated airflow tests and the room temperature air flow tests have good agreement. At the lowest Reynolds numbers (Re ≈ 196 and Re ≈ 250), the average Nusselt numbers were very close in value. For the heated air and Re ≈ 196, the average Nusselt number was 1.98 ± 0.18. The average Nusselt number was 1.88 ± 0.28 for the room temperature case. At the higher Reynolds numbers (Re ≈ 725 and Re ≈ 841), the room temperature case measured higher average Nusselt numbers, but also had a higher Reynolds number compared to the heated flow case. Additionally there was greater variability between tests for the room temperature results at the highest flow condition. The uncertainty in the mean for the highest Reynolds numbers were 0.86 and 0.35 for the room temperature and heated flows, respectively.

The correlation ($Nu = 0.08558\ Re^{0.5886}$) and the Nusselt numbers from the heated and room temperature flow cases are presented in Fig. 4. The standard error of fit is also presented as the shaded region around the line. As expected, the majority of the data is within the bounds of one standard deviation of the fit away from the line of best fit. When this region is expanded to two standard deviations of the fit, only one data point is outside of the bounds. This correlation and

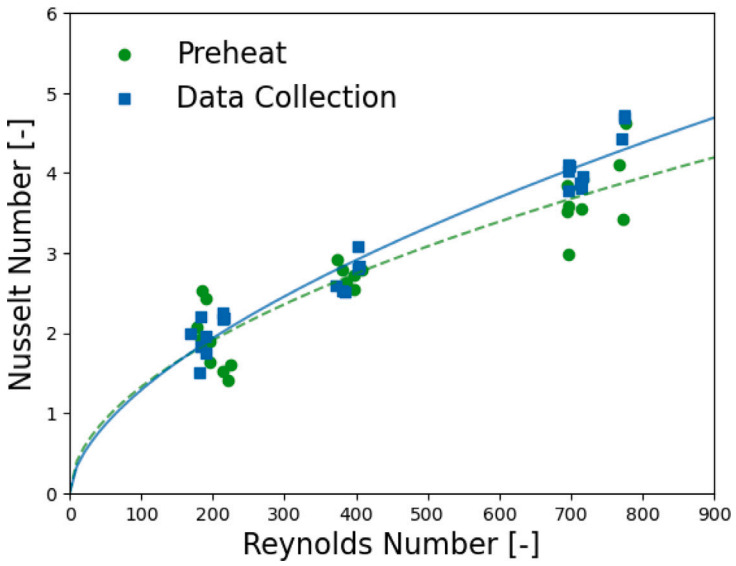

Fig. 3. Comparison of the Nusselt numbers for a single surrogate firebrand on a platform at different Reynolds numbers for the preheat and data collection periods during experiments. The solid blue line is a power law line of best fit (Nu = 0.08558 $Re^{0.5886}$) for the Nusselt numbers from the data collection. The dashed green line is the power law fit (Nu = 0.1189 $Re^{0.5238}$) for the preheat data. (For interpretation of the references to color in this figure legend, the reader is referred to the web version of this article.)

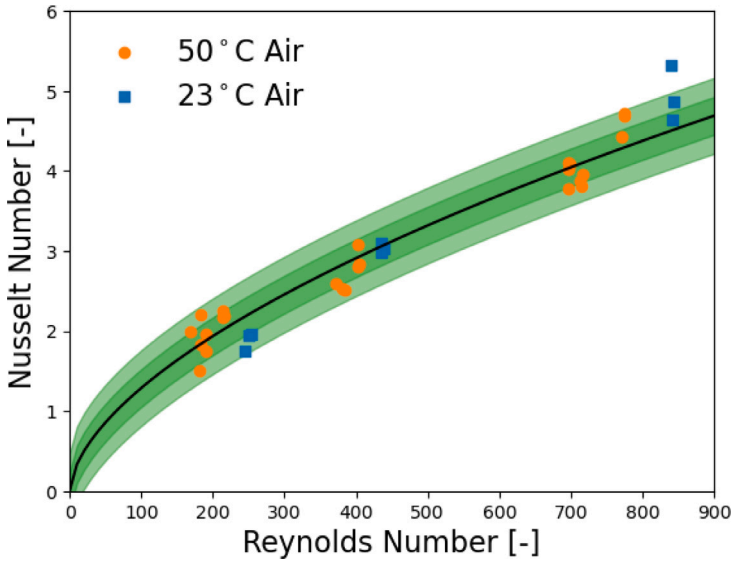

Fig. 4. Comparison of the Nusselt numbers from a single surrogate firebrand on a platform at different Reynolds numbers for two different air flow temperatures. 23 °C indicates the tests conducted at room temperature. The air was heated to 50 °C for the heated flow tests. The black line is best fit determined for the heated data set of the form, $Nu = aRe^b$. The shaded regions represents the standard error of fit. The larger shaded region in the lighter green color is 2 standard deviations of the fit from the line of best fit. The smaller shaded region in the darker green color is one standard deviation of the fit away from the line of best fit in either direction. (For interpretation of the references to color in this figure legend, the reader is referred to the web version of this article.)

the uncertainty bands were formed only using the heated flow data, and there is still good agreement with the room temperature data. Only one room temperature data point was outside of the two standard deviations of the fit. If all of the data including the room temperature data points were used for the correlation, there is only a small change in the correlation. From this analysis, we can see that the heated air flow over the naphthalene specimens allows for the convective heat transfer to be characterized given the preheating time is accounted for. This configuration differs from a cylinder in cross flow due to the cylinder resting on a flat plate. However it would be interesting to compare the heat transfer coefficients for these two configurations to see how the presence of the flat plate affects the heat transfer. Using the correlation by Churchill and Bernstein for a cylinder in cross flow for Re = 100 to 900, Nusselt numbers would range between approximately 3.3 and 9.3. On average, these values are about twice that of a single cylinder resting on a flat plate based on the correlation in this study. Using traditional correlations for a cylinder in cross flow from the literature would significantly overestimate the convective transfer.

One of the benefits of using a heated air flow in naphthalene sublimation experiments is the decrease in time required to have sufficient naphthalene mass loss. Based on the correlation by Ambrose, Lawrensen, and Sprake [15], the vapor pressure naphthalene increases by a factor of ten when the temperature is increased from 23 °C to 50 °C. This means the naphthalene will sublimate at a much faster rate in the heated flow cases. Based on the experimental mass loss rates, depending on flow condition and air flow temperature, there was significant difference in the time required for a given amount of mass loss. To illustrate this point, Table 1 shows the times required for 0.05 g of naphthalene mass loss for the different cases based on the mass loss rates measured in the experiments. From the values,

Table 1
Time required for 0.05 g of naphthalene mass loss for a given flow condition and air flow temperature.

Reynolds number	Temperature (°C)	Time required (min)
250	23	273
196	50	23
436	23	156
391	50	16
841	23	90
725	50	11

we can see that the heated flow cases take between 9%–12% of the time required for the room temperature tests. Based on the vapor pressure curve for naphthalene, the time required for the 50 °C air flow cases to sublimate the same amount of mass is approximately 10% of the time required for the room temperature (23 °C) air flow cases at nominally the same flow condition. Simply heating the air to 50 °C drastically decreases the amount of time required to run an experiment. Even considering the small amount of heating time required, the test time is still much shorter than it would be in a room temperature air experiment. With shorter test times, more tests can be conducted in the same period of time that would be needed for room temperature experiments. This could lead to more experiments for a given configuration, therefore decreasing the uncertainty associated with the measurement. Another advantage would be increasing the number of configurations tested allowing for results that are applicable over a wider range of experimental conditions.

3.2. Pile of three surrogate firebrands

Experiments were conducted for piles of three surrogate firebrands under four heated air flow conditions. The Nusselt numbers were calculated for each surrogate firebrand in the pile and for the whole pile. First we consider the Nusselt numbers for each individual firebrand in the pile shown in Fig. 5. From this plot we can see that the surrogate firebrand at the top of the pile (position 3) had the highest heat transfer coefficients. The surrogate firebrand on the bottom and on the downstream side (position 2) experienced the lowest heat transfer. On average, the Nusselt number at position 2 was about a third of the Nusselt number at position 3 for the same flow speed. Using the data for each individual firebrand, power law correlations were optimized for each firebrand position in the pile. Positions 1 and 3 have similar shapes in their curves, but the magnitude of the Nusselt numbers is lower. It is also interesting to note that the exponent on the Reynolds number in these two correlations is close to 0.5, which is often used for tube banks with low Reynolds numbers [17].

In addition to the individual surrogate firebrand Nusselt number correlations, there is some correlation relating the Reynolds number to the global heat transfer in the pile. For this analysis, the Nusselt numbers for the individual firebrand were averaged for each experiment, so the Nusselt number is still defined by the diameter of an individual firebrand. These global Nusselt numbers can be seen in Fig. 6. Additionally, a line of best fit using the power law form was found for the global Nusselt number. Here the Nusselt number takes the form $0.0659\ Re^{0.5572}$. The majority of the data is contained within the region of one standard deviation away from the line of best fit. The remaining data is included if the region is expanded to two standard deviations.

Finally, we compare the single surrogate firebrand heat transfer to the heat transfer in the firebrand pile configuration. All Nusselt numbers were defined using the diameter of a single firebrand, which allows for direct comparison between the two configurations. Fig. 7 shows the Nusselt numbers and correlations for the experiments with a single surrogate firebrand and the firebrand in position 1 in the pile configuration. The single firebrand and the firebrand in position 1 are in the same exact location of the platform used in these experiments. They are both located in the first groove, 25 mm from the leading edge of the platform. From this comparison, we can see that the single firebrand experiences higher heat transfer than the surrogate firebrand in position 1 of the pile at all of the flow conditions in these experiments. This is most likely due to the decreased airflow on the top and back side of the position 1 firebrand. The firebrand in position 3 blocks some of the air that would flow over the top of the position 1 firebrand if there was no obstacle. Additionally the firebrand at position 2 impedes the airflow to the back side of the position 1 firebrand. The Nusselt number represents the average heat transfer over the entire surface of the firebrand, so these areas with lesser air flow are included. This likely leads to the lower Nusselt number at position 1 in the firebrand pile compared to the single firebrand even though they are at the same location in space. On average, the position 1 firebrand in the pile was a factor of 1.5 lower than the single firebrand.

The correlations for the firebrands at the three different positions within the pile, the average global firebrand pile, and the single firebrand Nusselt number are presented in Fig. 8. Looking at the individual position Nusselt numbers, the position 1 firebrand Nusselt number is approximately the average of the position 2 and 3 firebrands Nusselt numbers. The global firebrand pile Nusselt number is the average of the Nusselt numbers at the three positions, so this leads to a value similar to position 1. Comparing the two highest heat transfer correlations, the single firebrand and the position 3 firebrand, we see that at lower Reynolds numbers (less than about 300), the Nusselt numbers are very similar. The average Nusselt number for the position 3 firebrand was 1.1 times lower than the single firebrand. However as flow speed increases, the Nusselt number correlations begin to diverge and the single firebrand experiences more heat transfer. It is possible that the air flow at the bottom portion of the position 3 firebrand encounters less air flow than the single firebrand. The position 1 and 2 firebrand contact the position 3 firebrand at a higher location on sides of the cylinder than the grooves in the platform. This could lead to decreased airflow in this region. Another possibility is that the concentration of naphthalene in the air flowing over the surrogate firebrands is no longer zero/negligible after passing over the position 1 firebrand meaning the approximation in Eq. (2) no longer holds. As the naphthalene at the surface of the position 1 sublimates, the mass fraction of naphthalene in the air increases and the potential for naphthalene sublimation decreases at position 3. In this case, accounting for the naphthalene already in the air would lead to higher transfer coefficients. The analogous heat transfer phenomena would be the air in the thermal boundary layer heating up as it flows over the pile. Similar effects with the reduced airflow and the presence of naphthalene in the freestream air were experienced by the position 2 firebrand. This firebrand experienced Nusselt numbers that were on average a factor of 3.4 lower than the single firebrand.

Generally, the single firebrand has the highest Nusselt number of the configurations/positions in these experiments. However, if the total convective heat transfer to the surroundings were considered, the firebrand pile would have higher total heat transfer due to having three times as many firebrands as the single firebrand. In the range of Reynolds numbers valid for these experiments, the Nusselt number for the single firebrand is not three times that of the global firebrand pile.

4. Conclusions

Naphthalene sublimation is a useful experimental technique to quantify the convective heat transfer, especially in cases with complex geometry or boundary conditions. In these experiments, naphthalene sublimation was used to characterize the convective heat transfer from a single surrogate firebrand resting on a flat plate and a pile of three surrogate firebrands resting on a flat plate. For the single surrogate firebrand, it was determined that $Nu = 0.08558\ Re^{0.5886}$ for the Reynolds numbers tested in these experiments ($Re \approx 160–850$).

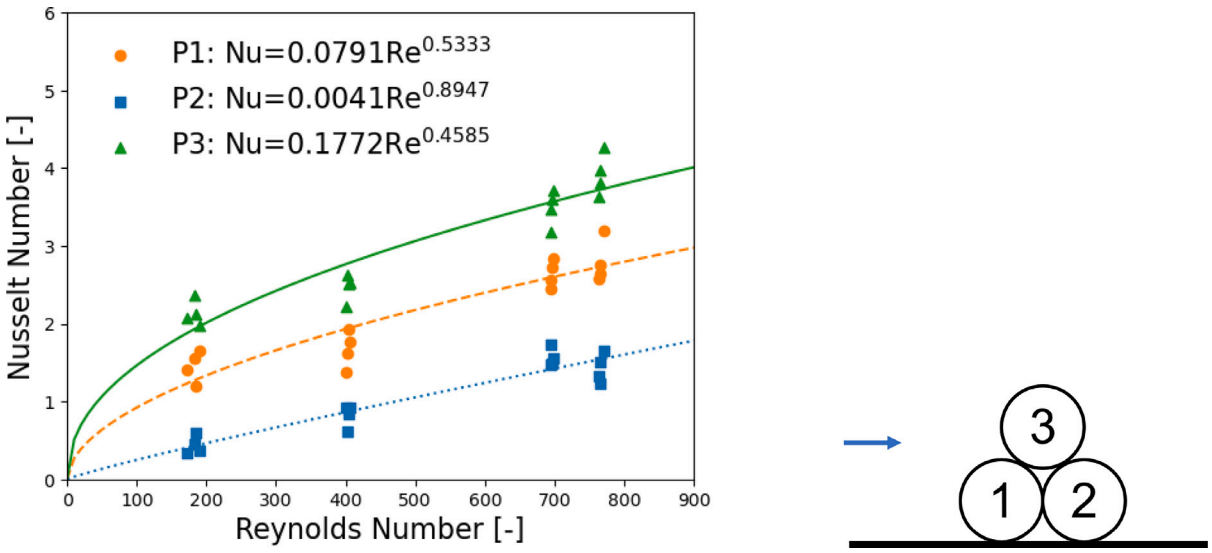

Fig. 5. Comparison of the individual Nusselt numbers for the surrogate firebrands in a pile configuration. The equations in the legend are lines of best fit for the given surrogate firebrand. The image to right shows a side view of the pile configuration with numbers indicating the different firebrand positions in the pile. The blue arrow indicates the air flow direction. (For interpretation of the references to color in this figure legend, the reader is referred to the web version of this article.)

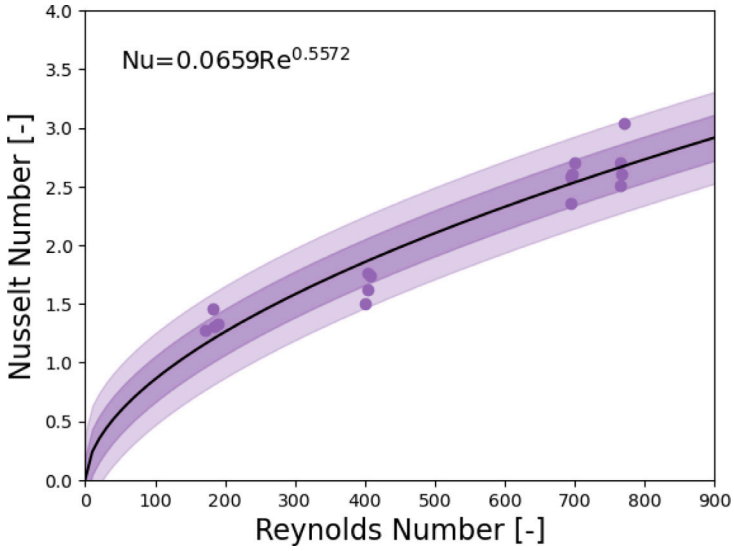

Fig. 6. Comparison of the global Nusselt number for three surrogate firebrands in a pile. The black line is best fit determined for the heated data set of the form, $Nu = aRe^b$. The shaded regions represents the standard error of fit. The larger shaded region in the lighter purple color is 2 standard deviations of the fit from the line of best fit. The smaller shaded region in the darker purple color is one standard deviation of the fit away from the line of best fit in either direction. (For interpretation of the references to color in this figure legend, the reader is referred to the web version of this article.)

Generally naphthalene sublimation experiments are often conducted at room temperature over long periods of time to ensure sufficient naphthalene sublimation. However, by increasing the temperature of the airflow to approximately 50 °C, the experimental duration was decreased while still having the desired amount of naphthalene sublimation. When using a heated flow, it is important to consider the temperature of the naphthalene cylinder when it is placed in the flow. A preheating period is necessary to ensure the correct transfer coefficients are calculated for the given experiment. In the experiments presented in this paper, we found that a ten minute preheat time allowed for the accurate determination of the transfer coefficients. To asses the validity of the heated air flow approach, additional tests were conducted at room temperature. There was good agreement between the Nusselt numbers derived from the heated and room temperature experiments. Additionally, the time required for the same amount of naphthalene mass loss decreased by a factor of ten when the airflow was increased from 23 °C to 50 °C. This would allow for more data to be collected in the same amount time needed for experiments conducted under room temperature conditions. Overall there are clear benefits from collecting data in naphthalene sublimation experiments with a heated air flow.

Additional tests were conducted in the heat air flow with simplified piles of three surrogate firebrands. Correlations were presented for the firebrands in a pile, both globally and individually. The firebrand at the top of the firebrand pile had the highest Nusselt numbers of those in the pile. The surrogate firebrand at the bottom on the downstream edge exhibited the lowest amount of mass transfer, and therefore the lowest Nusselt numbers. The average global Nusselt number correlation for the firebrand pile was $Nu = 0.0659\ Re^{0.5572}$. The results from the firebrand pile experiments were compared to the single surrogate firebrand experiments. Comparing the single firebrand to the firebrand at the same spatial location on the platform, but in the pile configuration, showed that the single firebrand had higher heat transfer coefficients.

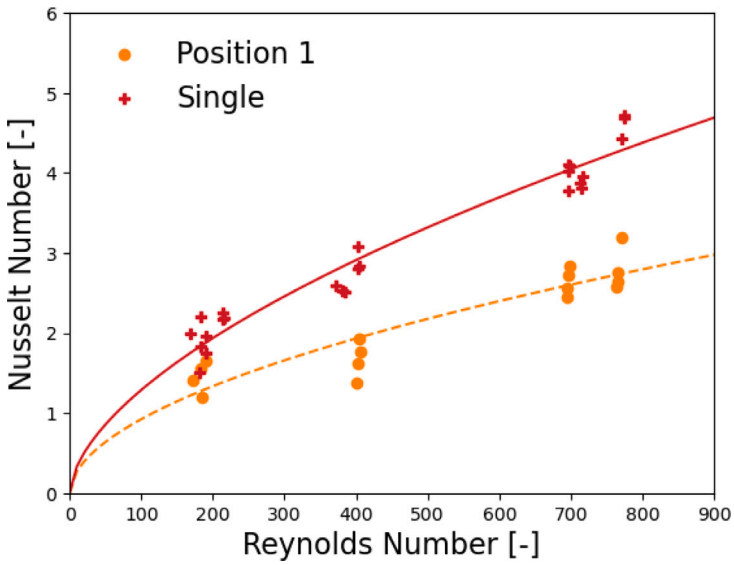

Fig. 7. Comparison of convective heat transfer for the single surrogate firebrand and the surrogate firebrand in position 1 of the pile configuration. Individual experiments are indicated with marker, and the lines represent the correlations based on the power law best fits for the data sets.

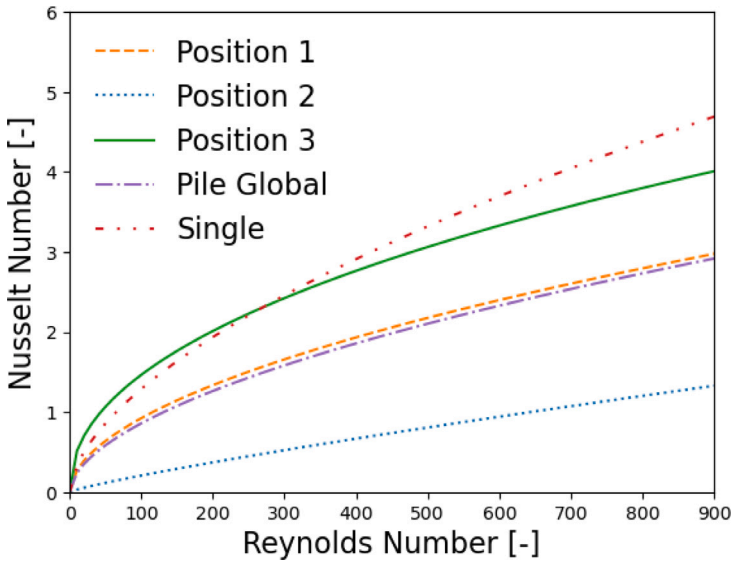

Fig. 8. Comparison of the correlations relating Reynolds numbers to Nusselt numbers for the single firebrand, individual firebrands within a pile, and the global firebrand pile. Correlations are the same as those presented in Figs. 4, 5, and 6.

At lower flow velocities, the firebrand at the top of the pile saw similar Nusselt numbers to the singular firebrand. However at higher air flows, the single firebrand experienced more convective heat transfer than the firebrand at the top of the pile. In general, the single firebrand had higher Nusselt numbers than those in the firebrand pile. However the difference was not enough that a single firebrand would have higher total convective heat transfer than the three firebrands combined in the pile configuration.

By studying the convective heat transfer of individual firebrands and piles of firebrands deposited on a surface, we can improve our understanding of the hazards associated with firebrand deposition and ignition. We could also better model and predict the heat transfer processes occurring during deposition and possible ignition events. Moving forward, other configurations such as firebrands of different shapes and aspect ratios should be considered. Additionally, different piles structures and spacing should be investigated to explore their effects on the convective heat transfer from a firebrand.

Declaration of competing interest

The authors declare that they have no known competing financial interests or personal relationships that could have appeared to influence the work reported in this paper.

Data availability

Data will be made available on request.

References

[1] Alexander Maranghides, William E. Mell, A case study of a community affected by the Witch and Guejito Fires, NIST Technical Note 1635, National Institute of Standards and Technology, Gaithersburg, MD, 2009.

[2] Russell Graham, Mark Finney, Chuck McHugh, Jack Cohen, Dave Calkin, Rick Stratton, Larry Bradshaw, Ned Nikolov, Fourmile Canyon fire findings, Gen. Tech. Rep. RMRS-GTR-289, US Department of Agriculture, Forest Service, Rocky Mountain Research Station, Fort Collins, CO, 2012.

[3] Luís M. Ribeiro, André Rodrigues, Davi Lucas, Domingos Xavier Viegas, The impact on structures of the pedrógão grande fire complex in June 2017 (Portugal), Fire 3 (4) (2020) 57.
[4] Mohamad El Houssami, Eric Mueller, Alexander Filkov, Jan C. Thomas, Nicholas Skowronski, Michael R. Gallagher, Kenneth Clark, Robert Kremens, Albert Simeoni, Experimental procedures characterising firebrand generation in wildland fires, Fire Technol. 52 (3) (2016) 731–751.
[5] Samuel L. Manzello, Thomas G. Cleary, John R. Shields, Alexander Maranghides, William Mell, Jiann C. Yang, Experimental investigation of firebrands: generation and ignition of fuel beds, Fire Saf. J. 43 (3) (2008) 226–233.
[6] Savannah S. Wessies, Michael K. Chang, Kevin C. Marr, Ofodike A. Ezekoye, Experimental and analytical characterization of firebrand ignition of home insulation materials, Fire Technol. 55 (3) (2019) 1027–1056.
[7] Karina Meerpoel-Pietri, Virginie Tihay-Felicelli, Paul-Antoine Santoni, Determination of the critical conditions leading to the ignition of decking slabs by flaming firebrands, Fire Saf. J. 120 (2021) 103017.
[8] Oleg Matvienko, Denis Kasymov, Egor Loboda, Anastasia Lutsenko, Olga Daneyko, Modeling of wood surface ignition by wildland firebrands, Fire 5 (2) (2022) 38.
[9] Franz Richter, Bryce Bathras, Julia Barbetta Duarte, Michael J. Gollner, The propensity of wooden crevices to smoldering ignition by firebrands, Fire Technol. (2022) 1–22.
[10] James L. Urban, Jiayun Song, Simon Santamaria, Carlos Fernandez-Pello, Ignition of a spot smolder in a moist fuel bed by a firebrand, Fire Saf. J. 108 (2019) 102833.
[11] Samuel L. Manzello, Sayaka Suzuki, Experimental investigation of wood decking assemblies exposed to firebrand showers, Fire Saf. J. 92 (2017) 122–131.
[12] Sayaka Suzuki, Samuel L. Manzello, Experimental investigation of firebrand accumulation zones in front of obstacles, Fire Saf. J. 94 (2017) 1–7.
[13] P.R. Souza Mendes, The naphthalene sublimation technique, Exp. Therm Fluid Sci. 4 (1991) 510–523.
[14] R.J. Goldstein, H.H. Cho, A review of mass transfer measurements using naphthalene sublimation, Exp. Therm Fluid Sci. 10 (4) (1995) 416–434, http://dx.doi.org/10.1016/0894-1777(94)00071-F, Experimental methods in Thermal and Fluid Science.
[15] D. Ambrose, I.J. Lawrenson, C.H.S. Sprake, The vapour pressure of naphthalene, J. Chem. Thermodyn. 7 (12) (1975) 1173–1176, http://dx.doi.org/10.1016/0021-9614(75)90038-5, URL https://www.sciencedirect.com/science/article/pii/0021961475900385.
[16] Pauli Virtanen, Ralf Gommers, Travis E. Oliphant, Matt Haberland, Tyler Reddy, David Cournapeau, Evgeni Burovski, Pearu Peterson, Warren Weckesser, Jonathan Bright, Stéfan J. van der Walt, Matthew Brett, Joshua Wilson, K. Jarrod Millman, Nikolay Mayorov, Andrew R.J. Nelson, Eric Jones, Robert Kern, Eric Larson, C.J. Carey, İlhan Polat, Yu Feng, Eric W. Moore, Jake VanderPlas, Denis Laxalde, Josef Perktold, Robert Cimrman, Ian Henriksen, E.A. Quintero, Charles R. Harris, Anne M. Archibald, Antônio H. Ribeiro, Fabian Pedregosa, Paul van Mulbregt, SciPy 1.0 Contributors, SciPy 1.0: Fundamental algorithms for scientific computing in Python, Nature Methods 17 (2020) 261–272, http://dx.doi.org/10.1038/s41592-019-0686-2.
[17] J.H. Lienhard IV, J.H. Lienhard, A Heat Transfer Textbook, fourth ed., Dover Publications, Mineola, NY, 2011, URL http://ahtt.mit.edu.